

ULRR

Multiwavelength Q-switched pulse operation with gold nanoparticles as saturable absorber

Item Type	Article
Authors	Li, Shi;Yin, Yu;Lewis, Elfed;Farrell, Gerald;Tokurakawa, Masaki;Rosol, Ahmad Haziq Aiman;Harun, Sulaiman Wadi;Wang, Pengfei
Citation	Optical Engineering;58 (6)
Publisher	Society of Photo-Optical Instrumentation Engineers (SPIE)
Download date	2026-05-12 00:41:43
Item License	https://creativecommons.org/licenses/by-nc-sa/1.0/
Link to Item	https://hdl.handle.net/10344/8924

Optical Engineering

OpticalEngineering.SPIEDigitalLibrary.org

Multiwavelength Q-switched pulse operation with gold nanoparticles as saturable absorber

Shi Li
Yu Yin
Elfed Lewis
Gerald Farrell
Masaki Tokurukawa
Ahmad Haziq Aiman Rosol
Sulaiman Wadi Harun
Pengfei Wang

SPIE

Shi Li, Yu Yin, Elfed Lewis, Gerald Farrell, Masaki Tokurukawa, Ahmad Haziq Aiman Rosol, Sulaiman Wadi Harun, Pengfei Wang, "Multiwavelength Q-switched pulse operation with gold nanoparticles as saturable absorber," *Opt. Eng.* **58**(6), 066104 (2019), doi: 10.1117/1.OE.58.6.066104.

Multiwavelength Q-switched pulse operation with gold nanoparticles as saturable absorber

Shi Li,^a Yu Yin,^a Elfed Lewis,^b Gerald Farrell,^c Masaki Tokurukawa,^d Ahmad Haziq Aiman Rosol,^e Sulaiman Wadi Harun,^e and Pengfei Wang^{a,f,*}

^aHarbin Engineering University, College of Science, Key Laboratory of In-Fiber Integrated Optics of Ministry of Education, Harbin, China

^bUniversity of Limerick, Optical Fiber Sensors Research Centre, Department of Electronic and Computer Engineering, Limerick, Ireland

^cTechnological University Dublin, Photonics Research Centre, Dublin, Ireland

^dUniversity of Electro-Communications, Institute for Laser Science, Tokyo, Japan

^eUniversity of Malaya, Photonic Engineering Lab, Department of Electrical Engineering, Faculty of Engineering, Kuala Lumpur, Malaysia

^fShenzhen University, College of Optoelectronic Engineering, Key Laboratory of Optoelectronic Devices and Systems of Ministry of Education and Guangdong Province, Shenzhen, China

Abstract. A multiwavelength Q-switched pulse operation obtained directly using a Tm-doped fiber laser and employing gold nanoparticles (GNPs) as a saturable absorber (SA material) is reported. The GNPs SA exhibits a modulation depth of 5.4% and a nonsaturable loss of 21.3%. Due to the saturable absorption and the high nonlinearity, dual-wavelength and triple-wavelength Q-switched pulse operations are obtained at pump power levels of 200 and 500 mW. To the best of our knowledge, this is the first ever reported use of GNPs as SA in multiwavelength Q-switched lasing generation. © 2019 Society of Photo-Optical Instrumentation Engineers (SPIE) [DOI: [10.1117/1.OE.58.6.066104](https://doi.org/10.1117/1.OE.58.6.066104)]

Keywords: gold nanoparticles SA; multiwavelength fiber laser; Q-switched pulse.

Paper 190492 received Apr. 11, 2019; accepted for publication May 14, 2019; published online Jun. 8, 2019.

1 Introduction

Multiwavelength pulse fiber lasers have developed rapidly in numerous application fields, including sensing, spectral ranging, optical communication, medical treatment, and material processing in the past few decades.¹ Furthermore, their operation wavelength bands cover a large range, including operation at 1.0, 1.5, and 2.0 μm .^{2–5} Compared with 1.0 and 1.5 μm multiwavelength pulse fiber lasers, multiwavelength pulse fiber lasers operating at 2.0 μm show great promise for use in many applications, including optical communications, optical sensing (given their inherent advantages of eye safe operation), and low loss in atmospheric transmission applications.⁴ However, compared to lasers operating in the 1.0 and 1.5 μm multiwavelength regions, pulse operation in the 2.0- μm region is more difficult to achieve due to the added requirements for more precise parameters (e.g., nonlinearity and the net dispersion) and a higher demand on the real SA materials (e.g., bandgap requirements).

Along with the development of the multiwavelength fiber lasers, numerous approaches have been reported to achieve pulse operation. These approaches are mainly based on the employment of an artificial saturable absorber (SA)^{6–10} and a real SA.^{3,4,11–16} A real SA is considered one of the most efficient methods for multiwavelength pulse generation. Numerous real SA materials have been studied for multiwavelength pulse generation including topological insulators,¹⁴ various transition metal dichalcogenides,^{3,4} black phosphorus¹⁷ etc. Graphene is a typical real SA material, which is widely used in the laser field and has proved popular for generating multiwavelength pulses in fiber lasers.^{11–13} However, graphene exhibits low damage threshold and demands complex fabrication, which has hindered development to date.¹³ Although the real SAs mentioned above have their own

set of unique advantages, their common drawback is weak optical stability, including low damage threshold and long-term instability, which is has been a major barrier in their successful development. To overcome this difficulty, researchers have focused on the use of metallic nanoparticles as the basis of an SA, as they can provide a stable output spectrum.¹⁸

Metal nanoparticles, whose diameters are less than 100 nm, have been receiving significant attention ranging from fundamental research to industrial production due to their outstanding physical properties such as large third-order nonlinearity and broad absorption, which mainly arise from the surface plasmon resonance (SPR) effect.^{18–22} SPR is an increasingly important optical phenomenon especially in the area of surface based chemical sensing, which is related with the coherent oscillations of electron plasmas at the surfaces of metallic particles.²³ Many unique nonlinear optical responses benefit from the adoption of the SPR effect using metal nanoparticles, such as surface-enhanced Raman scattering etc.²³ As a result of this range of valuable properties, metal nanoparticles have been widely applied many application fields such as life sciences, environmental monitoring, molecular recognition etc.²³ Gold nanoparticles (GNPs) represent a widely used and typical metal nanoparticle that has been widely studied in the past few years.^{24–26} By measuring the nonlinear optical response using the Z-scan technique,²⁴ GNPs have been identified as a highly suitable candidate as SAs because of their applicability in the case of the SPR effect. In the case of GNPs, their third-order nonlinear coefficient has been determined to be as high as $\sim 10^{-6}$, which is higher than that of graphene.²⁴ Their excellent nonlinear optical properties mean GNPs have much greater potential to achieve Q-switched or mode-locked pulse laser operation.

*Address all correspondence to Pengfei Wang, E-mail: pengfei.wang@dit.ie

Used as an SA, GNPs have been successfully introduced into the fiber laser cavity in order to achieve pulse operation as expected.^{25,26} Recently reported progress^{25,26} has meant that GNPs have attracted significant attention and are a promising candidate for enhancement of optical nonlinear effects, which means that they clearly have a potentially important role to play within the general application fields of nonlinear optics. However, to date the authors of this article are unaware of any reported work relating to multiwavelength pulse generation with GNPs used as an SA incorporated within the fiber laser cavity.

In this paper, multiwavelength Q-switched pulse operation is reported for a Tm-doped fiber (TDF) laser employing GNPs as a high-performance SA material. The GNPs SA exhibited a modulation depth of 5.4% and a nonsaturable loss of 21.3%. Due to a combination of the high saturable absorption and a high degree of nonlinearity, dual-wavelength and triple-wavelength Q-switched pulse operation was obtained using a pump power of 200 and 500 mW, respectively. To the best of our knowledge, this is the first ever reported use of GNPs as SA in multiwavelength Q-switched lasing generation.

2 Fabrication and Characterization of the GNPs Thin-Film SA

The GNPs was prepared initially with an addition of 50 mL TSC (trisodium citrate, $\text{Na}_3\text{C}_6\text{H}_5\text{O}_7$), 3 mL sodium-4-styrene-sulfonate, and 3 mL of NaBH_4 in a beaker containing 1000 mL deionised water (DI water, resistivity 18.0 $\text{M}\Omega$) while stirring at 450 rpm (rotations per minute). 50 mL HAuCl_4 (chloroauric acid, 5 mM, in water) was added dropwise (~ 2 mL/min) into the mixture with continuous stirring followed by the addition of an excess amount of TSC (20 mL). The reaction was allowed to take place for 5 min before the mixture was placed in a centrifuge as the cleaning step to remove any particulate matter. The aqueous medium

containing the GNPs ended up with a magenta color [Fig. 1(a) inset]. The resulting magenta solution shows no further color change. Then the solution containing the GNPs was mixed with polyvinyl alcohol (PVA) solution to fabricate the SA film. The PVA solution was prepared by dissolving PVA powder (MFCD00081922, Sigma Aldrich) into 80 mL of DI water, which was then stirred at 145°C until the powder completely dissolved. The GNPs and PVA were mixed and slowly stirred for a further 2 h using a magnetically actuated stirrer. The resulting suspension was then poured into the petri dish and left to dry at room temperature. After 2 days, the thin film was slowly peeled from the petri dish. At that point, the GNPs-PVA film was ready and the end product is clearly signed by yellow circle in Fig. 1(a).

The morphology of the GNP film was examined using a scanning electron microscope (SEM), whereas the size of the GNPs was measured using transmission electron microscopy (TEM) while. Figures 1(b) and 1(c) show the morphology and sizes and of GNPs observed from the SEM and TEM images, respectively. The spherical shape plasmonic GNPs have an average size ~ 5.46 nm. Because of their spherical morphology, the GNPs provide great physical and chemical stability and can coexist within the film. They do not tend to agglomerate, hence preventing any decrease in surface energy prior to stabilization by the PVA film. The GNP-PVA film was then cut into a square film (1 mm \times 1 mm \times 0.01 mm) to attach onto an FC/PC fiber ferrule as shown in Fig. 1(d). The ferrule was then matched with another fresh ferrule via a fiber adaptor after depositing a small amount of index matching liquid onto the fiber end to form an all-fiber SA device. It is worth noting that FC/PC connectors contain a spring mechanism to make sure that in a normal fiber-fiber connection, the two fiber cores are pressed together with just enough force to make gentle physical contact. In this case when the film is introduced, the same connector spring mechanisms work to minimize

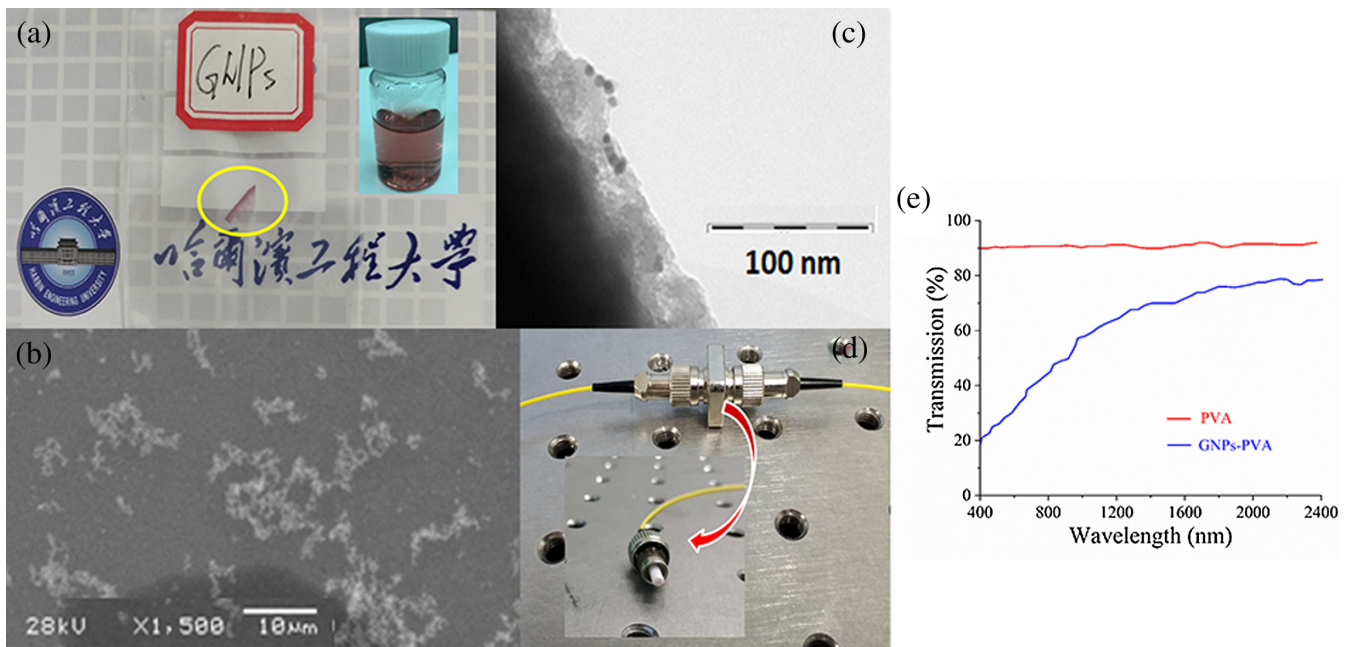


Fig. 1 Characteristic of the GNPs. (a) Photograph of the GNPs film; inset: photograph of GNPs aqueous solution, (b) SEM image of the GNPs, (c) TEM image of the GNPs, (d) fiber-compatible SA device with GNPs film, and (e) linear transmission of the GNPs-PVA versus wavelength.

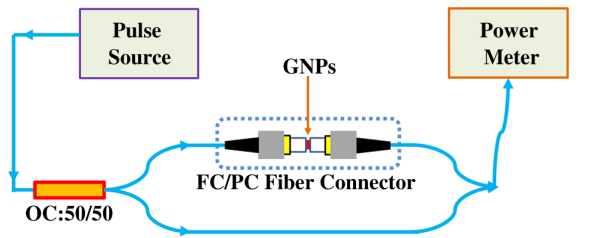


Fig. 2 Setup of measurement of saturable absorption of the GNPs by balance twin-detector measurement technique.

the pressure placed on the film by the fiber/ferrule ends. The insertion loss of GNPs-PVA SA device was measured to be about 2.8 dB. The optical transmission spectrum of the GNPs-PVA film was measured and is shown in Fig. 1(e). In addition, the transmission spectrum of the PVA is also shown for comparison. It is clear that the transmission increases with wavelength. Finally, the transmission of the GNPs-PVA film at the wavelength of 1895 nm was about 75.1%.

The nonlinear optical properties of the GNPs PVA film were also investigated using a balanced twin-detector measurement technique³, whose setup is shown schematically in Fig. 2. The illumination pulse was generated using a picosecond fiber laser source (wavelength, 1.94 μm; pulse duration, ~3.6 ps; repetition rate, ~22 MHz). The nonlinear transmission of the film was measured by comparing the input power and output power values using a two-channel powermeter (PM320E). As shown in Fig. 3, the fabricated film exhibits the classical saturable absorption characteristic in that the transmission initially increases with the incident pulse peak intensity and then levels out. The modulation depth and nonsaturable loss of the film were measured as ~5.4% and ~21.3%, respectively, and the former is shown in Fig. 3. It is worth noting that no nonlinear response was measured in the case for the same experiment conducted using only a pure PVA film, devoid of GNPs, confirming that the saturable absorption property solely originates from the GNPs.

3 Experimental Setup

Figure 4 shows the schematic diagram of the multiwavelength Q-switched Thulium-doped fiber laser (TDFL) with

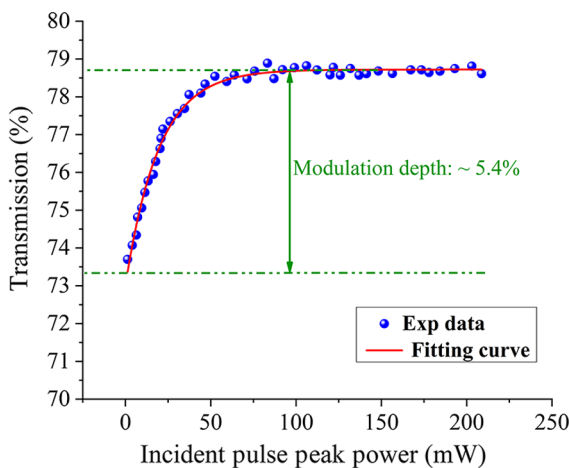


Fig. 3 The nonlinear optical properties of GNP film by balance twin-detector measurement technique.

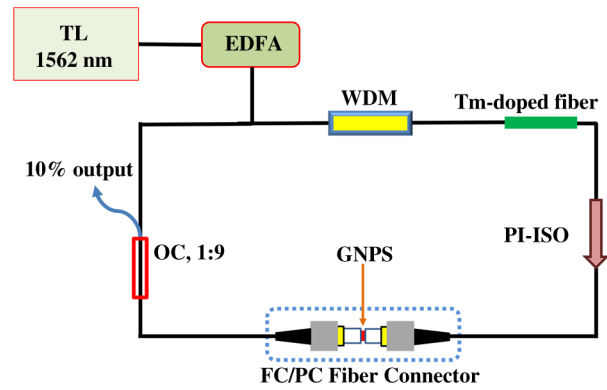


Fig. 4 Schematic diagram of the experimental setup.

a GNP-based SA. The pumping source consists of a tunable laser (Santec TSI-710) with a center wavelength of 1562 nm to provide the pump light, and an erbium-doped fiber amplifier (EDFA, MC-EDFA-230), which produced the amplified light output signal. The pump source provided a maximum output power of 700 mW, which was used to pump the gain medium, the 5-m long TDF (Nufern SM-TSF-9/125) was

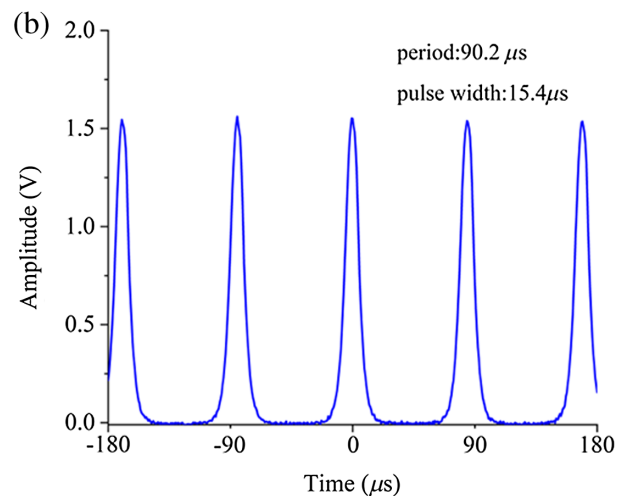
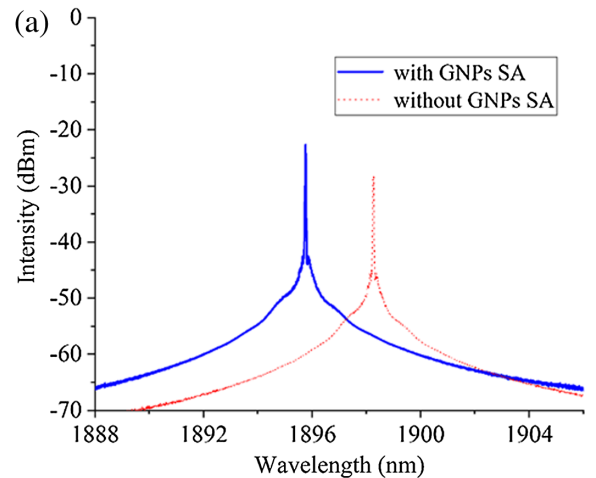


Fig. 5 Characteristic of the single Q-switched pulse with threshold pumping power of 187 mW. (a) Optical spectrum and (b) typical oscilloscope pulse waveform.

optically coupled to the pump via a wavelength division modulator (WDM) (MCWDM-15/19). The generated photons then propagated into the polarization-independent isolator (PI-ISO, MCI-1980) pigtailed with a standard single mode fiber (SMF-28) of $8.3\ \mu\text{m}$ core diameter. In the designed laser cavity, the PI-ISO not only maintained unidirectional operation but also decreased the possibility of any Brillouin backscattering, which could potentially disturb the stability of pulsed operation.²⁷ The GNPs SA was introduced into the lasing cavity between the PI-ISO and a 10-dB optical coupler (OC, 1980-FBT-C). The 90% port of the optical coupler was spliced with the WDM to complete the ring cavity. The 10% port was connected with the optical spectral analyzer (OSA, YOKOGAWA, AQ-6370C) to measure the laser's output spectrum. The time-resolved pulsed laser output signal was measured using a digital storage oscilloscope (Tektronix MDO4054-6). In the ring cavity in this experiment, no polarization controller was used in order to exclude the any combined effect from in-cavity polarization manipulation and the pump power, to allow confirmation that the nonlinearity of the GNPs is the only possible cause of the multiwavelength output pulse generation.³

4 Results and Discussion

Before placing the GNPs SA into the laser cavity, continuous wave lasing was achieved using a pump threshold power of 136 mW. No pulse like output was measured in this cavity when the pumping power was gradually increased to a maximum value of 700 mW. The GNPs SA was inserted into the laser cavity as shown in Fig. 4. A Q-switched pulse with

single wavelength operation was obtained at the pump threshold power of 187 mW. The resulting spectra were compared in Fig. 5(a) at the threshold pump power value, with the blue line representing the cavity with GNPs SA included and the red line is without GNPs SA. As shown in Fig. 5, the laser operated at a center wavelength of 1898.2 nm with an extinction ratio of 20.5 dB and 1895.8 nm with extinction ratio 21.7 dB with and without the SA, respectively. The incorporation of the SA therefore results in a shift of the output spectrum to a shorter wavelength, the shift being 2.4 nm. This clearly observable shift was attributed to the additional insertion loss resulting from the introduction of the SA. The extinction ratio of blue line (SA included) is a little higher, which was due to the existence of higher gain being achieved at the shorter wavelength.²⁴ At the pump power of 187 mW, the typical oscilloscope (OSC) pulse waveform was recorded by the oscilloscope as shown in Fig. 5(b). The repetition rate and pulse width were 11.1 kHz and $15.4\ \mu\text{s}$, respectively.

As the pump power was further increased to 200 mW, dual-wavelength Q-switched pulse operation was clearly observed. The typical spectrum and oscilloscope pulse waveform recorded by the OSA and OSC are shown in Figs. 6(a) and 6(b), respectively. The two peaks of the dual-wavelengths are located at 1895.8 and 1897.2 nm. The extinction ratios of the two peaks are 34.5 and 36 dB, respectively. Compared with the single pulse at the lower pump power of 187 mW, the dual-wavelength laser produced a higher extinction ratio. This indicates that the dual-wavelength Q-switched pulse operation state achieves much higher gain.

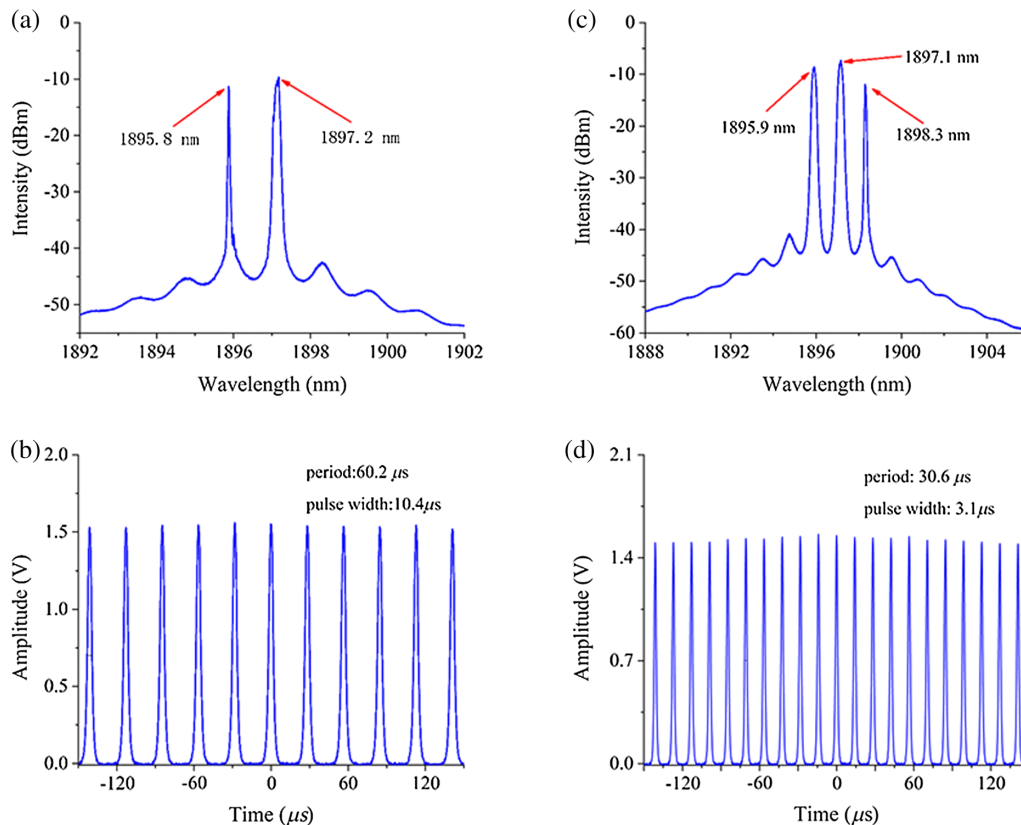


Fig. 6 Characteristic of the multiwavelength Q-switched pulse. (a) Optical spectrum at 200 mW, (b) typical oscilloscope pulse waveform at 200 mW, (c) optical spectrum at 500 mW, and (d) typical oscilloscope pulse waveform at 500 mW.

The repetition rate was measured as 16.6 kHz. The individual pulse width was 10.4 μs , which is shown in Fig. 6(b). In the lasing cavity, the surface plasmon resonance property of GNPs can be equivalent to a two-level structure of the plasmon resonance ground state and plasmon excited states.²⁵ As the incident light intensity increases, the resonant excited state of the plasmon gradually reaches the saturated absorption state, similar to the saturation absorption of a real SA. Therefore, the presence of GNPs is a key factor for obtaining the pulse operation by acting as an effective SA within the laser cavity. Furthermore, the high-nonlinearity of GNPs excites the four-wave mixing effect that not only has the capacity to suppress mode competition in the TDF but also combines with the gain of the TDF to produce the multi-wavelength output.²³

As the pumping power was further increased to 500 mW, triple-wavelength Q-switched output was achieved. The three peaks of the triple-wavelength are located at 1895.9, 1897.1, and 1898.3 nm, which are clearly shown in Fig. 6(c). The three extinction ratios were measured as 36.15, 37.44, and 32.9 dB, respectively. The repetition rate was measured as 32.7 kHz. The individual pulse width was 3.1 μs , which is clearly shown in Fig. 6(d). As the pumping power was increased, the high-nonlinearity of the GNPs more effectively suppressed the mode competition in the TDF, and furthermore combined with the higher gain of the TDF to produce the greater number of output wavelengths peaks. A comparison of the output pulse characteristics resulting from the 200- and 500-mW pump power cases clearly shows that more spectral pulses with narrower pulse duration in the same time period could be observed in the 500-mW case. The higher pump power forces the GNPs to saturate faster, which is a key factor leading to the time-resolved pulse width reduction, which therefore generate more pulses in the same time period in combination with a narrower pulse width.²⁸ No distinct amplitude modulation could be observed in any envelope of the pulse exhibited in Figs. 6(b) and 6(d), which indicated that the pulse train is a typical feature of passive Q-switching with weak self-mode locking.^{18,19}

Finally, the pump power was further increased to a maximum value of 700 mW, at which value no further wavelength peaks were observed. The repetition rate and pulse width were recorded continuously throughout the duration of this experiment using the OSC. The variation of the repetition rate and pulse width versus the pump power were recorded and presented in Fig. 7(a). The green region in Fig. 7(a) is the dual-wavelength case, which is characterized by a repetition rate range of 16.6 to 32.7 kHz and pulse width range of 10.4 to 3.1 μs . The yellow region represents the triple-wavelength case, which is characterized by a repetition rate range of 32.7 to 155.27 kHz and pulse width range of 2.1 μs to 805 ns. The variation of repetition rate and pulse width agrees well with that predicted by Q-switching theory with SA present.¹⁸ The presence of the output pulse was dependent on the light intensity propagating through the GNPs SA. In a weakly excited state, the electrons are excited to conduction state when the photons are absorbed into the GNPs. In the strong excitation state, the ground state ions are depleted, and the excited state is fully occupied, and hence the absorption reaches saturation.²⁹ The pulse is generated when the in-cavity energy exceeds saturation absorption threshold. The repetition rate is dependent on the stored energy, which is

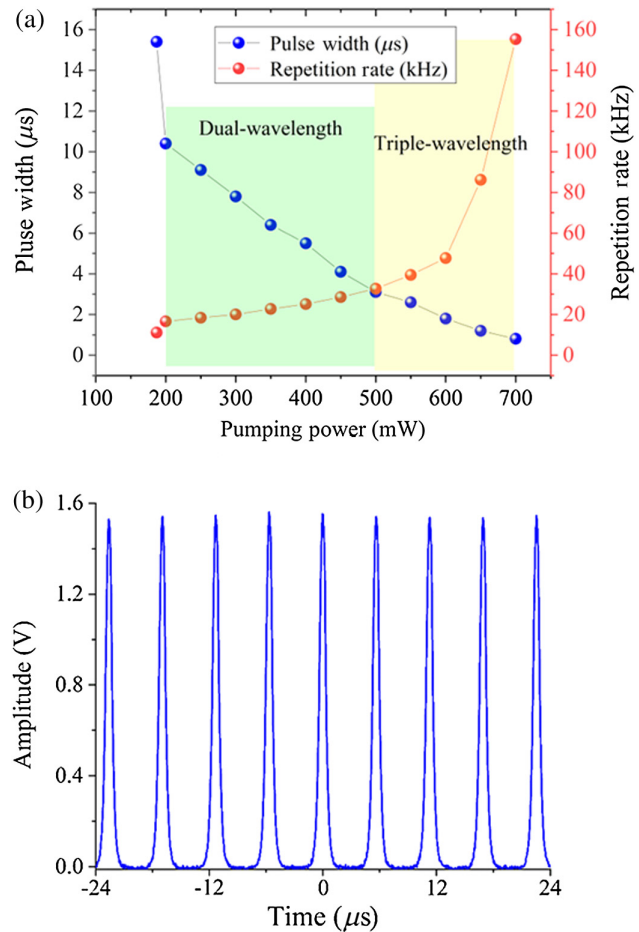


Fig. 7 (a) The variation trend of repetition rate and pulse width with the pumping power. (b) Typical oscilloscope pulse waveform at 700 mW.

ultimately determined by the pump power.²⁵ Hence, the increase in repetition rate varies as the pump power increases. Meanwhile, with increasing pump power, more atoms accumulate in the upper energy level of the gain medium when the SA recovers, which accelerates establishment and extinction of the pulse to generate a narrower width pulse.¹⁸ The pulse duration was 805 ns at the pumping power 700 mW, which is shown in Fig. 7(b). In the experimental, the GNPs-PVA film plays the role of SA device in the laser cavity with a maximum output power of 700 mW, which indicates that the damaged threshold of GNPs-PVA SA-based laser device is much better than that of graphene.¹¹⁻¹³

In order to confirm the long-term stability of the GNPs-based TDFL, the emission spectra of the Q-switched laser were measured every 1 h for a total duration of continuous operation of 5 h. The emission spectra are shown in Fig. 8(a). Neither the center wavelength or peak spectral intensity was observed to vary within the accuracy of the recording instrumentation (OSA) of this investigation. The results therefore demonstrate that the Q-switched lasing is stable based on the GNPs SA. Furthermore, the performance of the Q-switched fiber laser was measured to confirm the longer stability of the GNPs SA, which is a key factor for future practical implementations. The output lasing was observed every day for 1 week. During the entire observation period, the threshold of Q-switched lasing exhibited no change, which was expected

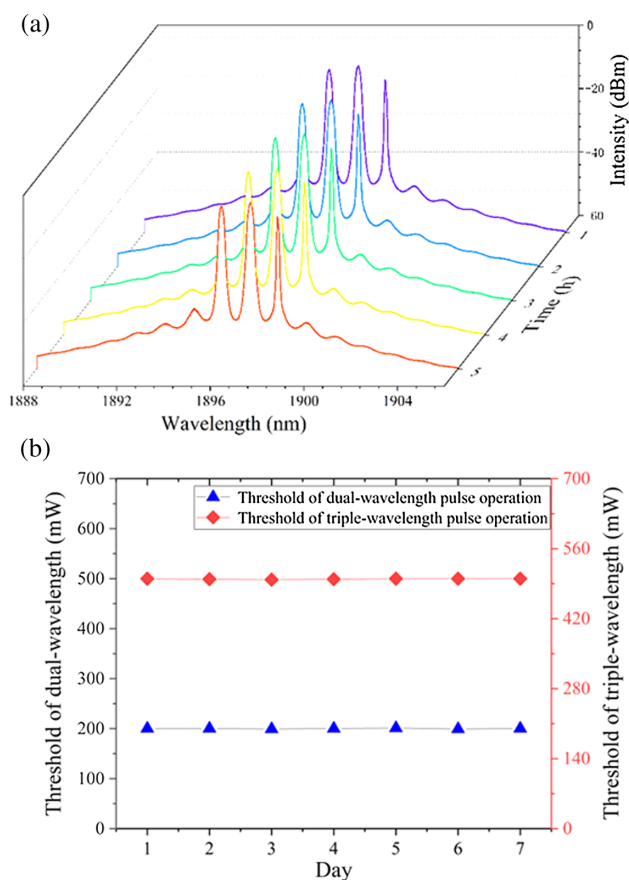


Fig. 8 Characteristics of the GNPs stability. (a) Measured emission spectra of the Q-switched laser based on the GNPs SA at pumping power of 500 mW. (b) Measured thresholds of dual-wavelength and triple-wavelength pulse operation for 1 week.

as the thresholds of dual-wavelength and triple-wavelength pulse operation also exhibit no change [shown in Fig. 8(b)]. The stability of the laser for short- and long-term indicated the long-term stability of the multiwavelength Q-switched fiber laser with GPNs SA is an excellent candidate for future use in a wide range of applications.

5 Conclusion

In conclusion, an all fiber multiwavelength passively Q-switched TDFL based on the GNPs SA has been successfully fabricated and demonstrated. The essential enhanced nonlinear optical properties introduced by the GNPs through an enhanced SPR effect greatly benefit the operating characteristics and performance of this device. By inserting the GNPs into the laser cavity, single wavelength passively Q-switched laser behavior was observed at the threshold pump power of 187 mW. Dual-wavelength and triple-wavelength operations were obtained at pump powers of 200 and 500 mW, respectively. The pulse duration was observed to decrease from 15.4 μ s to 805 ns and the repetition rate to increase from 11.1 to 155.27 kHz over the range of pump power excitation. Long-term stability tests (lasting many weeks) have shown the device exhibits excellent stability with no discernible drift of the output power, wavelength, or Q-switching threshold during the full duration of these tests. The achieved experimental results indicate that the GNPs SA can be

used for constructing multiwavelength pulsed lasers near the 2.0- μ m wavelength region.

Acknowledgments

The work was supported by National Key R&D Program of China under Grant No. 2016YFE0126500; the National Natural Science Foundation of China (NSFC) under Grant No. 615750502; The fundamental research funds for the central universities under Grant No. HEUCFG201841; Key Program for Natural Science Foundation of Heilongjiang Province of China under Grant No. ZD2016012; Open Fund of the State Key Laboratory on Integrated Optoelectronics under Grant No. IOSKL2016KF03, this work was also supported by the 111 project (B13015) to the Harbin Engineering University.

References

- U. Keller, "Recent developments in compact ultrafast lasers," *Nature* **424**(6950), 831–838 (2003).
- H. Zhang and J. Liu, "Gold nanobipyramids as saturable absorbers for passively Q-switched laser generation in the 1.1 μ m region," *Opt. Lett.* **41**(6), 1150–1152 (2016).
- S. Li et al., "A microfiber knot incorporating a tungsten disulfide saturable absorber based multi-wavelength mode-locked erbium-doped fiber laser," *J. Lightwave Technol.* **36**, 5633–5639 (2018).
- R. Woodward et al., "Wideband saturable absorption in few-layer molybdenum diselenide (MoSe₂) for Q-switching Yb-, Er- and Tm-doped fiber lasers," *Opt. Express* **23**(15), 20051–20061 (2015).
- Y. Jia and F. Chen, "Compact solid-state waveguide lasers operating in the pulsed regime: a review," *Chin. Opt. Lett.* **17**(1), 012302 (2019).
- D. Noske et al., "Dual-wavelength operation of a passively mode-locked 'figure-of-eight' ytterbium-erbium fibre soliton laser," *Opt. Commun.* **108**(4–6), 297–301 (1994).
- L. Yun, X. Liu, and D. Mao, "Observation of dual-wavelength dissipative solitons in a figure-eight erbium-doped fiber laser," *Opt. Express* **20**(19), 20992–20997 (2012).
- Q.-Y. Ning et al., "Bright-dark pulse pair in a figure-eight dispersion-managed passively mode-locked fiber laser," *IEEE Photonics J.* **4**(5), 1647–1652 (2012).
- Z. Zhang, Z. Xu, and L. Zhang, "Tunable and switchable dual-wavelength dissipative soliton generation in an all-normal-dispersion Yb-doped fiber laser with birefringence fiber filter," *Opt. Express* **20**(24), 26736–26742 (2012).
- D. Mao and H. Lu, "Formation and evolution of passively mode-locked fiber soliton lasers operating in a dual-wavelength regime," *J. Opt. Soc. Am. B* **29**(10), 2819–2826 (2012).
- S. Huang et al., "Tunable and switchable multi-wavelength dissipative soliton generation in a graphene oxide mode-locked Yb-doped fiber laser," *Opt. Express* **22**(10), 11417–11426 (2014).
- Z. Luo et al., "Multiwavelength mode-locked erbium-doped fiber laser based on the interaction of graphene and fiber-taper evanescent field," *Laser Phys. Lett.* **9**(3), 229–233 (2012).
- N. Zhao et al., "Dual-wavelength rectangular pulse Yb-doped fiber laser using a microfiber-based graphene saturable absorber," *Opt. Express* **22**(9), 10906–10913 (2014).
- M. Liu et al., "Dual-wavelength harmonically mode-locked fiber laser with topological insulator saturable absorber," *IEEE Photonics Technol. Lett.* **26**(10), 983–986 (2014).
- X. Zhao et al., "Switchable, dual-wavelength passively mode-locked ultrafast fiber laser based on a single-wall carbon nanotube modelocker and intracavity loss tuning," *Opt. Express* **19**(2), 1168–1173 (2011).
- X. Liu et al., "Versatile multi-wavelength ultrafast fiber laser mode-locked by carbon nanotubes," *Sci. Rep.* **3**, 2718 (2013).
- F. Rashid et al., "Using a black phosphorus saturable absorber to generate dual wavelengths in a Q-switched ytterbium-doped fiber laser," *Laser Phys. Lett.* **13**(8), 085102 (2016).
- T. Jiang et al., "Passively Q-switching induced by gold nanocrystals," *Appl. Phys. Lett.* **101**(15), 151122 (2012).
- Z. Kang et al., "Gold nanorods as saturable absorbers for all-fiber passively Q-switched erbium-doped fiber laser," *Opt. Mater. Express* **3**(11), 1986–1991 (2013).
- D. Fan et al., "Passively Q-switched erbium-doped fiber laser using evanescent field interaction with gold-nanosphere based saturable absorber," *Opt. Express* **22**(15), 18537–18542 (2014).
- X.-D. Wang et al., "Gold nanorod as saturable absorber for Q-switched Yb-doped fiber laser," *Opt. Commun.* **346**, 21–25 (2015).
- H. Ahmad et al., "Tunable 2.0 μ m Q-switched fiber laser using a silver nanoparticle based saturable absorber," *Laser Phys.* **27**(6), 065110 (2017).

23. Z. Kang et al., "Passively Q-switched erbium doped fiber laser using a gold nanostars based saturable absorber," *Photonics Res.* **6**(6), 549–553 (2018).
24. H. Liao et al., "Large third-order optical nonlinearity in Au:SiO₂ composite films near the percolation threshold," *Appl. Phys. Lett.* **70**(1), 1–3 (1997).
25. M. Ahmad et al., "Gold nanoparticle based saturable absorber for Q-switching in 1.5 μm laser application," *Laser Phys.* **27**(11), 115101 (2017).
26. X. Zhang et al., "Self-assembled gold nanoparticles as saturable absorber for low-threshold all-solid-state pulsed 2 μm laser," *Opt. Mater.* **83**, 82–86 (2018).
27. A. Latiff et al., "All-fiber dual-wavelength Q-switched and mode-locked EDFL by SMF-THDF-SMF structure as a saturable absorber," *Opt. Commun.* **389**, 29–34 (2017).
28. H. Huang et al., "Gold nanorods as the saturable absorber for a diode-pumped nanosecond Q-switched 2 μm solid-state laser," *Opt. Lett.* **41**(12), 2700–2703 (2016).
29. C. Pang et al., "Lithium niobate crystal with embedded au nanoparticles: a new saturable absorber for efficient mode-locking of ultrafast laser pulses at 1 μm ," *Adv. Opt. Mater.* **6**, 1800357 (2018).

Shi Li received his bachelor's degree from Jilin University, China, in 2015 and a master of optical engineering from Harbin Engineering University in 2017. He is currently pursuing his PhD in ultrashort pulse fiber laser at Harbin Engineering University.

Yu Yin received her bachelor's degree from Jilin University, China, in 2015 and is currently pursuing her PhD in fiber optics at the Harbin Engineering University.

Elfed Lewis works as a professor in Optical Fiber Sensors Research Centre, Department of Electronic and Computer Engineering, University of Limerick. His research interests include compound

glass materials, computational photonics, and photonic devices and applications.

Gerald Farrell works as a professor in the Photonics Research Centre, Technological University Dublin. His research interests include fiber sensors, computational photonics, photonic devices, and applications development.

Masaki Tokurukawa works as an associate professor at the Institute for Laser Science, University of Electro-Communications. His research interests include fiber lasers and high-power lasers.

Ahmad Haziq Aiman Rosol is currently pursuing his PhD in fiber lasers at the Faculty of Engineering, University of Malaya.

Sulaiman Wadi Harun received his BEng degree in electrical and electronics system engineering from Nagaoka University of Technology, Japan, in 1996 and MSc and PhD degrees in photonics from the University of Malaya in 2001 and 2004, respectively. Currently, he is a full professor at the Faculty of Engineering, University of Malaya. His research interests include fiber optic active and passive devices.

Pengfei Wang received his PhD in optics engineering from the Photonics Research Centre (PRC), Dublin Institute of Technology (DIT), Dublin, Ireland, in November 2008. He joined the College of Science, Harbin Engineering University, Harbin, China, as a full-time distinguished professor in 2015. His research interests include compound glass materials, fiber lasers, computational photonics, photonic devices, and applications development (optical communication and optical).